GAS SENSITIVITY OF NANOCRYSTALLINE COBALT DOPED NICKEL FERRITES

Hnin Hlwar Nu[1], Moe Min Min Aye[2], Win Kyaw[3] & Hla Hla Than[4]

Abstract

Gas sensing materials of Cobalt doped Nickel ferrites, $Ni_{1-x}Co_xFe_2O_4$ (x = 0.0, 0.1, 0.2 and 0.3) were prepared by self-combustion method. A quick combustion was taken as the calcination of metal hydroxides and the reaction between metal oxides. The obtained powders were pressed into disk shapes and subjected to thermal treatment at 1000°C for 30 min. The X-ray diffraction (XRD) analysis was carried out to investigate the crystalline phase formation. Microstructural properties of the samples were investigated by Scanning Electron Microscopy (SEM). The grain size of the samples was found to be varied with the dopant concentration of Co. It was investigated the sensitivities of the samples from the gas-sensitive electrical resistance measurements in acetone, ethanol, octane and liquid petroleum gas (LPG) atmospheres. It was observed that the gas sensitivity depends on the concentration of Co dopant and the test gases to be detected.

Keywords: Cobalt doped Nickel ferrites, self-combustion method, XRD, SEM, gas sensitivity

Introduction

Nanometer-sized materials, which have high surface activity due to their small particle size and enormous surface area, have been widely studied in the field of gas sensors in recent years [Harris, (2009); Kumar, (2009)]. In technologies where ferrites are to be used for magnetic or electrical applications, high-density materials are generally required and the ferrites are often prepared by high temperature solid-state reactions between finely ground powders. Although most applications of ferrites as ceramic materials require high densities to achieve the desired properties, there are many

----

[1]. Dr., Demonstrator, Department of Physics, Meiktila University
[2]. Dr., Lecturer, Department of Physics, University of Yangon
[3]. Dr., Associate Professor, Department of Physics, Sagaing University
[4]. Dr., Professor & HOD, Department of Physics, Meiktila University

applications for which lower densities and high surface area are preferred [Iyer, (2009); Pathan, (2010)].

Many ferrites are spinels with the formula AB_2O_4, where A and B represent various metal cations, usually including iron Fe. The magnetic material known as "NiFe" has the formula $NiFe_2O_4$, with Fe^{3+} occupying the octahedral sites and Ni^{2+} occupy the tetrahedral sites, it is an example of a spinel ferrite. Spinel ferrites usually adopt a crystal motif consisting of cubic close-packed (fcc) oxides (O^{2-}) with A cations occupying one eighth of the tetrahedral holes and B cations occupying half of the octahedral holes. If one eight of the tetrahedral holes are occupied by B cation, then one fourth of the octahedral sites are occupied by A cation and the other one fourth by B cation and it is called the inverse spinel structure [Marial, (2013); Sharma, (2005)]. In the present study, Nickel ferrite doped with small amounts of Cobalt was investigated as gas sensor. An attempt to improve the sensitivity and nanoparticles of Nickel ferrite have been partly replaced with Co on Ni and Fe, respectively.

Materials and Method

Preparation of Cobalt Doped Nickel Ferrites

In this work, nanocrystalline Cobalt Doped Nickel ferrites, $Ni_{1-x}Co_xFe_2O_4$ (where x = 0.0, 0.1, 0.2 and 0.3) were prepared by self-combustion method. Analytical Reagent (AR) grade Nickel (II) Nitrate Hexahydrate [$Ni(NO_3)_2.6H_2O$], Cobalt (II) Nitrate Hexahydrate [$Co(NO_3)_2.6H_2O$] and Iron (III) Nitrate Nonahydrate [$Fe(NO_3)_3.9H_2O$] were used as the raw materials. Ammonium Hydroxide [NH_4OH] was used as the fuel. The starting materials were weighed with desired stoichiometric compositions and mixed each others. The obtained precursor solution was heated on a hot plate at room temperature 29°C to 100°C for 1 h. Then, a quick combustion was taken as the calcination of metal hydroxides and the reaction between metal oxides. The obtained combustion powder was pressed into disk shape pellet and subjected to thermal treatment at 1000°C for 30 min in vacuum chamber (160 mmHg) using DELTA A Series Temperature Controller DTA4896. The K-type thermocouple was used as the temperature sensor for read-out the actual or real temperature in the chamber. Flow-diagram of the

preparation procedure of the Cobalt Doped Nickel ferrites using auto-combustion method is shown in Figure 1. Photographs of the sample preparation procedure are shown in Figures 2(a – p).

XRD Measurement

X-ray powder diffraction patterns of the $Ni_{1-x}Co_xFe_2O_4$ (where x = 0.0, 0.1, 0.2 and 0.3) samples were observed on a RIGAKU MULTIFLEX X-ray Powder Diffractometer using CuK_α radiation (λ = 1.54056 Å) in 2q range of 10° – 70°. The crystallite size was calculated by Scherrer's formula, using the full width at half maximum intensity for (311) plane of the pattern.
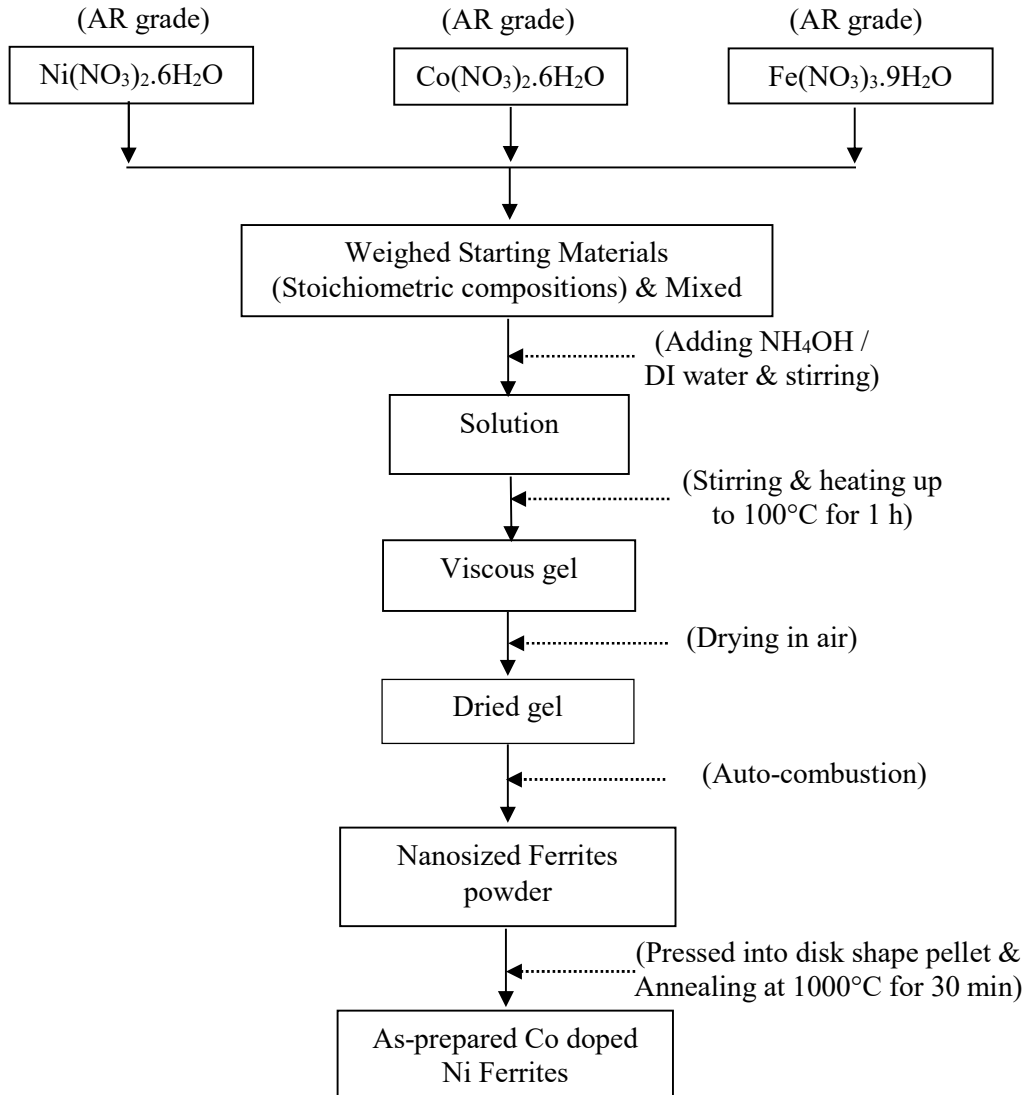
Figure 1. Flow-diagram of the preparation of Cobalt Doped Nickel ferrites

Figure 2. Photographs of the starting materials of (AR) grade (a) Ni(NO₃)₂.6H₂O and (b) Co(NO₃)₂.6H₂O
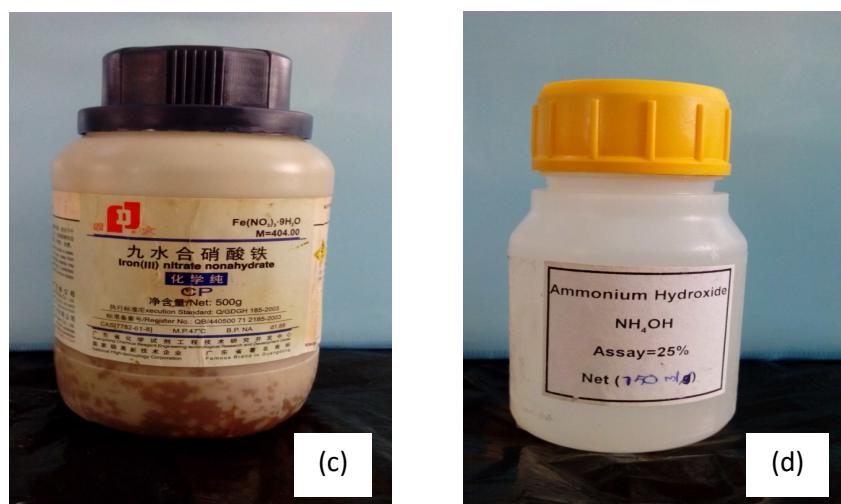
Figure 2. Photographs of the (c) starting materials of (AR) grade Fe(NO₃)₃.9H₂O and (d) NH₄OH

Figure 2. Photographs of the (e) weighed starting materials for x = 0.0 sample and (f) mixed solid solutions of starting materials for x = 0.0 sample
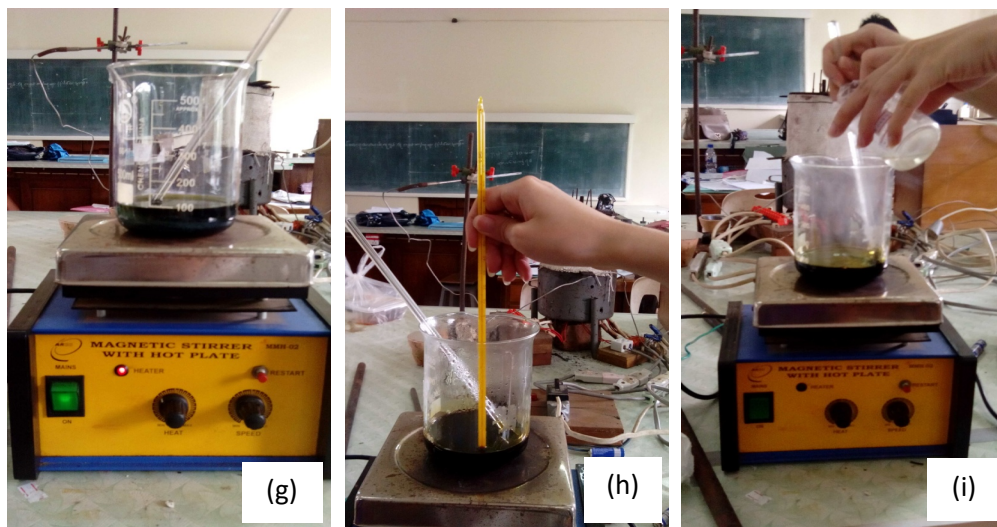
Figure 2. Photographs of the (g) heated and stirred of mixed solution of x = 0.0 sample using magnetic stirrer, (h) checked for solution temperature 100°C and (i) NH₄OH solution poured into heated solution
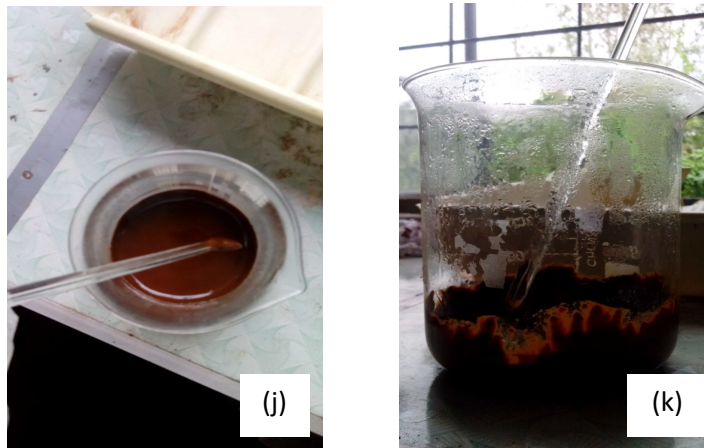
Figure 2. Photographs of the (j) top-view of x = 0.0 viscous gel and (k) side-view of combustion x = 0.0 ferrite
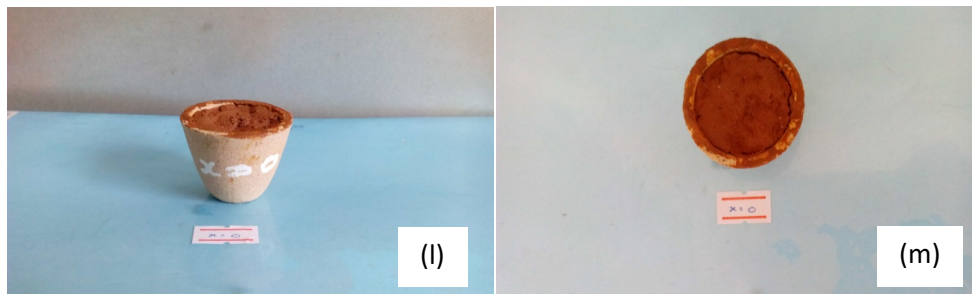
Figure 2. Photographs of the (l) side-view and (m) top-view of combustion x = 0.0 ferrite

Figure 2. Photographs of the (n) DELTA A Series Temperature Controller DTA4896 at 1000°C and (o) experimental setup of sample preparation system

Figure 2.(p) Photograph of the as-prepared $Ni_{1-x}Co_xFe_2O_4$ where x = 0.0 ferrite

SEM Measurement

In the present work, the morphological features of $Ni_{1-x}Co_xFe_2O_4$ (x = 0.0, 0.1, 0.2 and 0.3) powders were investigated by using JEOL JSM-5610LV SEM with the accelerating voltage of 15 kV, the beam current of 50 mA and 5500 times of photo magnification.

Gas Sensitive Electrical Resistance Measurement

The as-prepared Cobalt Doped Nickel ferrites, $Ni_{1-x}Co_xFe_2O_4$ (x = 0.0, 0.1, 0.2 and 0.3) samples were made pellets by SPECAC hydraulic pellet-maker using 5 ton (~70 MPa) to detect gas sensing effects of the samples. The silver paste (conductive pen) was made over the sample to ensure good electrical contacts. Ring-shaped copper electrodes were used to observe the electrical properties of the samples. The electrical resistances of the samples were observed in the ambient condition (air) and acetone, ethanol, octane and liquid petroleum gas (LPG) conditions. The electrical resistances of the samples were measured by using MASTECH digital multi-meter.

In the data collection, firstly, the electrical resistances were observed in air. For the gas sensing measurements, the sensor element (ferrite disk) was placed in a glass chamber. Gas sensing properties were investigated at room temperature. The experiments were performed with four test gases: acetone, ethanol, octane and liquid petroleum gas (LPG).

The sensitivity, S, defined as the ratio:

$$S = \frac{\Delta R}{R_a} = \frac{|R_a - R_g|}{R_a}$$

where R_a and R_g are the sensor resistances in air and in presence of the test gas, respectively.

Electrical resistances of the samples were observed by MASTECH digital multi-meter after the exposure times 3 min and 5 min respectively. Thickness and area of each of the sample were 3.33 mm and 1.14×10^{-4} m^2 respectively. Photographs of the experimental setup of gas sensitive electrical resistances measurements are shown in Figures (a – h) respectively.
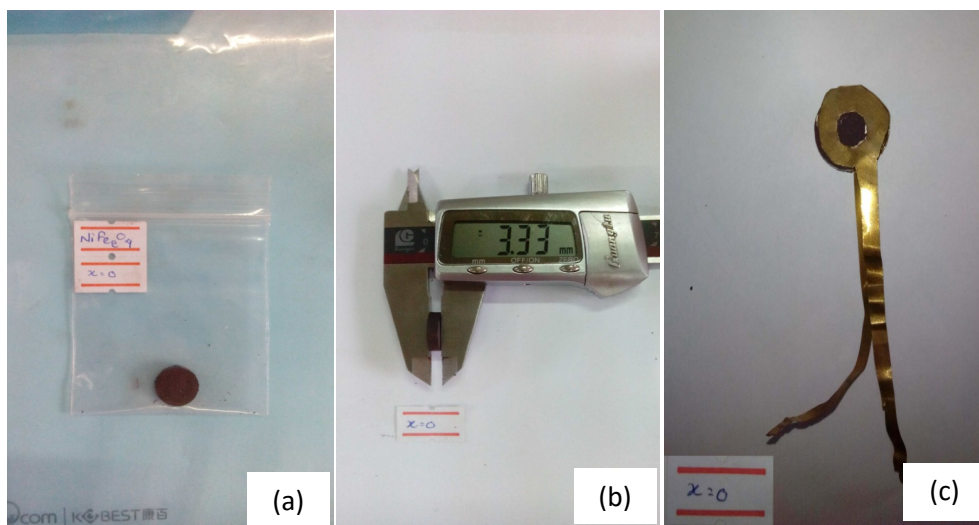
Figure 3. Photographs of the (a) $Ni_{1-x}Co_xFe_2O_4$ (x = 0.0) ferrite pellet, (b) thickness measurement of x = 0.0 sample pellet and (c) ring shape Cu electrode mounted on both-sides of the x = 0.0 sample
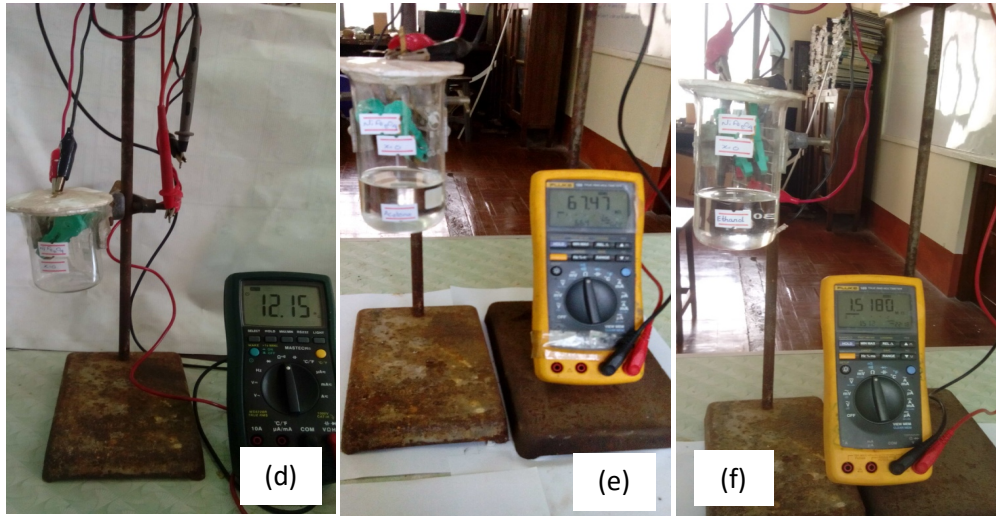
Figure 3. Photographs of the (d) experimental setup of gas-sensitive electrical properties measurements of x = 0.0 sample in air, (e) in acetone and (f) in ethanol atmospheres
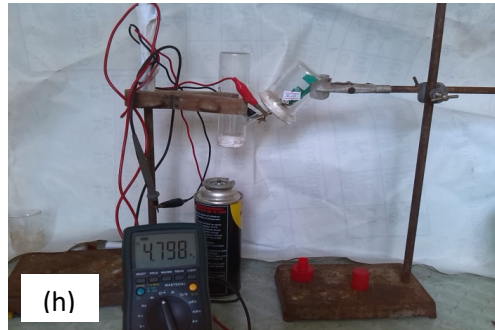
Figure 3. Photographs of the experimental setup of gas-sensitive electrical properties measurements of x = 0.0 sample (g) in octane and (h) in LPG atmospheres

Results and Discussion

X-Ray Diffraction Analysis

Powder X-ray diffraction patterns of $Ni_{1-x}Co_xFe_2O_4$ (x = 0.0, 0.1, 0.2 and 0.3) samples are shown in Figures 4(a – d). The observed XRD lines were identified by using standard JCPDS data library files of

(1) Cat. No. 86-2267> Trevorite – $NiFe_2O_4$ for $NiFe_2O_4$ or x = 0.0 sample and

(2) Cat. No. 86-2267> Trevorite – $NiFe_2O_4$ and Cat. No. 22-1086> $CoFe_2O_4$ – Cobalt Iron Oxide for $Ni_{0.9}Co_{0.1}Fe_2O_4$, $Ni_{0.8}Co_{0.2}Fe_2O_4$ and $Ni_{0.7}Co_{0.3}Fe_2O_4$.

As shown in Figure 4(a), five diffraction peaks at 2θ values of 30.275°, 35.639°, 43.319°, 57.397° and 62.905° corresponding to (220), (311), (400), (511) and (440) planes of the sample have been observed and compared with the JCPDS, Cat. No. 86-2267> Trevorite – $NiFe_2O_4$- spinel type cubic nickel ferrite phase - standard powder diffraction data file. The collected XRD pattern confirms / indicates that the resultant particles are $Ni_{1-x}Co_xFe_2O_4$ (x = 0.0) powder.

As shown in Figure 4(b), the collected diffraction lines were found to be agreed with the standard data file. The collected peaks in the sample are (220), (311), (400), (511) and (440) respectively. These lines indicated that the sample was mono-phase or single phase crystalline material.

As shown in Figure 4(c), they can be clearly seen that only the intense peaks of (220), (311), (222), (400), (511) and (440) planes were identified by the standard data files of the same in Cat. Nos. Others lines, e.g., the planes such as (111) and (422) as shown in library files were not identified because the library files were only pure/undoped ferrites materials. Thus, it may be assumed that some of the dopant atoms of Cd^{2+} substituted in the Mg^{2+} lattice sites, then the bond lengths of tetrahedral sites and octahedral sites can be varied due to the lattice substitution of the samples.

Also, as shown in Figure 4(d), six strongest peaks of (220), (311), (222), (400), (511) and (440) planes were identified with standard library files. The lowest intensity of the two lines (111) and (422) as shown in library files were not identified because the library files were only pure/undoped ferrites materials.

In the collected XRD patterns, the appearance of the diffraction peaks demonstrates the Cobalt Doped Nickel ferrites, $Ni_{1-x}Co_xFe_2O_4$ (x = 0.0, 0.1, 0.2 and 0.3) spinel samples. The experimental results of the samples are presented in Table 1(a – d). According to XRD patterns, the samples belong to cubic structure at room temperature. The lattice parameters were evaluated by using crystal utility of the equation $\dfrac{\sin^2\theta}{(h^2+k^2+l^2)}=\dfrac{\lambda^2}{4a^2}$ [5]. The strongest peak was found to be (311) reflection, which indicated the dominated plane of the polycrystalline phase.

The experimental results of the calculated average lattice parameters and the observed lattice parameters are tabulated in Table 2. Variation of the lattice parameters with the dopant concentration of Co is shown in Figure 5. As shown in Figure 5, the lattice parameters of the samples increased with increase in concentration of Co due to the ionic substitution of Co on Ni in the lattice sites. It can be simply explained that the ionic radii of Co^{2+} and Ni^{2+} are 0.82 Å and 0.78 Å, thus when the increase in dopant concentration of Co^{2+} on divalent cation sites of Ni^{2+}, then the lattice parameters of the unit cell of undoped $NiFe_2O_4$ increase.

The crystallite sizes of each of the samples were estimated by using the Scherrer formula, $D=\dfrac{0.9\lambda}{B\cos\theta}$, where "$D$" is the crystallite size (nm), "λ' is the wavelength of incident X-ray (Å), "θ" is the diffraction angle of the peak under consideration at FWHM (°) and "B" is the observed FWHM (radians). The ferrite peaks are quite broad as a consequence of the nanometre size of the crystallite domains.

In the present work, the average crystallite sizes are tabulated in Table 2. In the present work, the average crystallite sizes are tabulated in Table 3. The obtained average crystallite sizes are in the range 50.2421 nm – 73.5475 nm and it indicates the nanosized $Ni_{1-x}Co_xFe_2O_4$ (x = 0.0, 0.1, 0.2 and 0.3) ferrites or it can be said that the nanocrystalline materials. Variation of the crystallite sizes with the dopant concentration of Co of the samples is shown in Figure 5. It was found that the crystallite size of the samples decreased with the increase in dopant concentration of Co.
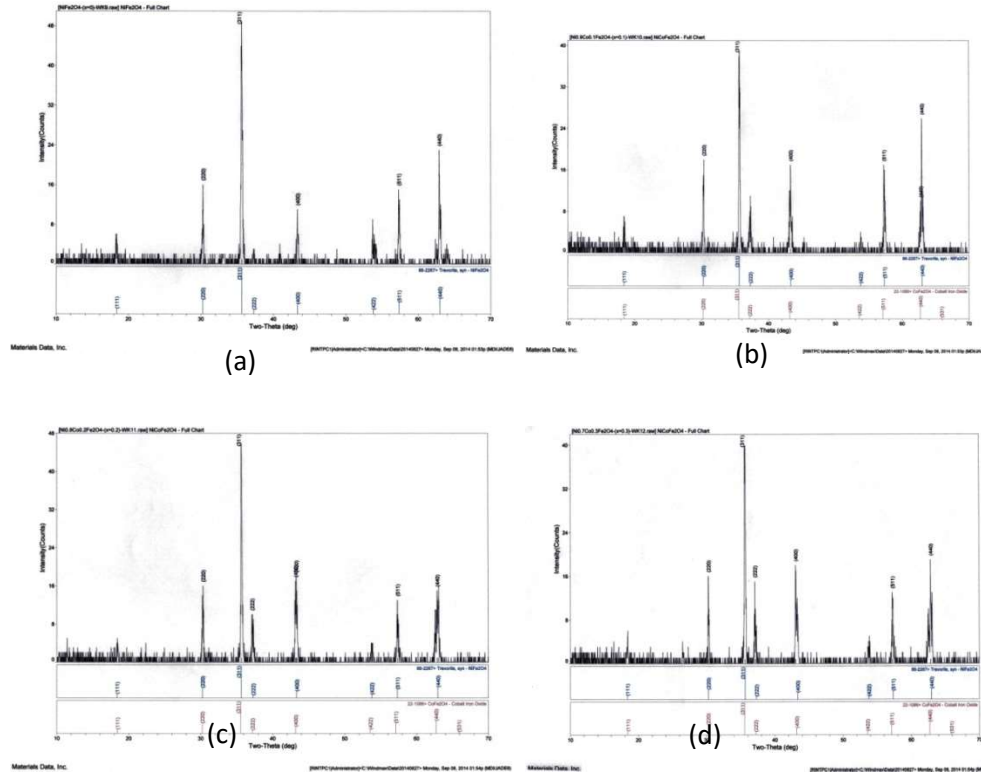
Figure 4. XRD patterns of $Ni_{1-x}Co_xFe_2O_4$ where (a) x = 0.0, (b) x = 0.1, (c) x = 0.2 and   (d) x = 0.3 ferrites

Table 1.(a) XRD data of $Ni_{1-x}Co_xFe_2O_4$ (where x = 0.0) ferrite

[NiFe2O4-(x=0)-WK9.raw] NiFe2O4 - Full Chart								Peak ID Report
SCAN: 10.0/70.0/0.02/0.06(sec), Cu(40kV,40mA), I(max)=49, 08/27/14 20:04								
PEAK: 11-pts/Quartic Filter, Threshold=1.0, Cutoff=0.0%, BG=1/0.5, Peak-Top=Summit								
NOTE: Intensity = Counts, 2T(0)=0.0(deg), Wavelength to Compute d-Spacing = 1.54056Å (Cu/K-alpha1)								
#	2-Theta	d(Å)	Height	Height%	Phase ID	d(Å)	I%	(h k l)	2-Theta	Delta
1	30.275	2.9497	16	32.7	Trevorite, syn	2.9476	29.6	(2 2 0)	30.298	0.022
2	35.639	2.5171	49	100.0	Trevorite, syn	2.5137	100.0	(3 1 1)	35.689	0.050
3	43.319	2.0870	11	22.4	Trevorite, syn	2.0842	20.3	(4 0 0)	43.378	0.060
4	57.397	1.6041	13	26.5	Trevorite, syn	1.6045	25.4	(5 1 1)	57.382	-0.015
5	62.905	1.4762	23	46.9	Trevorite, syn	1.4738	33.1	(4 4 0)	63.021	0.116

Line Shifts of Individual Phases:
    PDF#86-2267 - Trevorite, syn <2T(0) = 0.0, d/d(0) = 1.0>

Table 1.(b) XRD data of $Ni_{1-x}Co_xFe_2O_4$ (where x = 0.1) ferrite

[Ni0.9Co0.1Fe2O4-(x=0.1)-WK10.raw] NiCoFe2O4 - Full Chart									Peak ID Report
SCAN: 10.0/70.0/0.02/0.06(sec), Cu(40kV,40mA), I(max)=39, 08/27/14 19:59									
PEAK: 13-pts/Quartic Filter, Threshold=1.0, Cutoff=0.0%, BG=1/0.5, Peak-Top=Summit									
NOTE: Intensity = Counts, 2T(0)=0.0(deg), Wavelength to Compute d-Spacing = 1.54056Å (Cu/K-alpha1)									

#	2-Theta	d(Å)	Height	Height%	Phase ID	d(Å)	I%	(h k l)	2-Theta	Delta
1	30.330	2.9445	18	46.2	CoFe2O4	2.9470	30.0	(2 2 0)	30.304	-0.025
2	35.680	2.5143	39	100.0	Trevorite, syn	2.5137	100.0	(3 1 1)	35.689	0.009
3	43.304	2.0876	17	43.6	CoFe2O4	2.0888	20.0	(4 0 0)	43.278	-0.026
4	57.261	1.6076	17	43.6	CoFe2O4	1.6093	30.0	(5 1 1)	57.193	-0.068
5	62.774	1.4790	10	25.6	CoFe2O4	1.4783	40.0	(4 4 0)	62.805	0.031
6	62.937	1.4756	26	66.7	Trevorite, syn	1.4738	33.1	(4 4 0)	63.021	0.084

Line Shifts of Individual Phases:
PDF#86-2267 - Trevorite, syn <2T(0) = 0.0, d/d(0) = 1.0>
PDF#22-1086 - Cobalt Iron Oxide <2T(0) = 0.22, d/d(0) = 1.0>

Table 1.(c) XRD data $Ni_{1-x}Co_xFe_2O_4$ (where x = 0.2) ferrite

[Ni0.8Co0.2Fe2O4-(x=0.2)-WK11.raw] NiCoFe2O4 - Full Chart									Peak ID Report
SCAN: 10.0/70.0/0.02/0.06(sec), Cu(40kV,40mA), I(max)=46, 08/27/14 19:54									
PEAK: 13-pts/Quartic Filter, Threshold=1.0, Cutoff=0.0%, BG=1/0.5, Peak-Top=Summit									
NOTE: Intensity = Counts, 2T(0)=0.0(deg), Wavelength to Compute d-Spacing = 1.54056Å (Cu/K-alpha1)									

#	2-Theta	d(Å)	Height	Height%	Phase ID	d(Å)	I%	(h k l)	2-Theta	Delta
1	30.263	2.9509	14	30.4	Trevorite, syn	2.9476	29.6	(2 2 0)	30.298	0.035
2	35.664	2.5154	46	100.0	CoFe2O4	2.5159	100.0	(3 1 1)	35.657	-0.007
3	37.138	2.4189	10	21.7	CoFe2O4	2.4102	8.0	(2 2 2)	37.277	0.139
4	43.279	2.0888	18	39.1	CoFe2O4	2.0888	20.0	(4 0 0)	43.278	-0.001
5	57.340	1.6055	13	28.3	Trevorite, syn	1.6045	25.4	(5 1 1)	57.382	0.042
6	62.883	1.4767	15	32.6	CoFe2O4	1.4783	40.0	(4 4 0)	62.805	-0.078
7	63.104	1.4720	16	34.8	Trevorite, syn	1.4738	33.1	(4 4 0)	63.021	-0.083

Line Shifts of Individual Phases:
PDF#86-2267 - Trevorite, syn <2T(0) = 0.0, d/d(0) = 1.0>
PDF#22-1086 - Cobalt Iron Oxide <2T(0) = 0.22, d/d(0) = 1.0>

Table 1.(d) XRD data of $Ni_{1-x}Co_xFe_2O_4$ (where x = 0.3) ferrite

[Ni0.7Co0.3Fe2O4-(x=0.3)-WK12.raw] NiCoFe2O4 - Full Chart									Peak ID Report
SCAN: 10.0/70.0/0.02/0.06(sec), Cu(40kV,40mA), I(max)=40, 08/27/14 19:49									
PEAK: 13-pts/Quartic Filter, Threshold=1.0, Cutoff=0.0%, BG=1/0.5, Peak-Top=Summit									
NOTE: Intensity = Counts, 2T(0)=0.0(deg), Wavelength to Compute d-Spacing = 1.54056Å (Cu/K-alpha1)									

#	2-Theta	d(Å)	Height	Height%	Phase ID	d(Å)	I%	(h k l)	2-Theta	Delta
1	30.268	2.9504	16	40.0	Trevorite, syn	2.9476	29.6	(2 2 0)	30.298	0.030
2	35.621	2.5183	40	100.0	CoFe2O4	2.5159	100.0	(3 1 1)	35.657	0.035
3	37.082	2.4224	15	37.5	CoFe2O4	2.4102	8.0	(2 2 2)	37.277	0.194
4	43.300	2.0878	12	30.0	CoFe2O4	2.0888	20.0	(4 0 0)	43.278	-0.022
5	57.261	1.6076	12	30.0	CoFe2O4	1.6093	30.0	(5 1 1)	57.193	-0.068
6	62.880	1.4767	19	47.5	CoFe2O4	1.4783	40.0	(4 4 0)	62.805	-0.075

Line Shifts of Individual Phases:
PDF#86-2267 - Trevorite, syn <2T(0) = 0.0, d/d(0) = 1.0>
PDF#22-1086 - Cobalt Iron Oxide <2T(0) = 0.22, d/d(0) = 1.0>

Table 2. The lattice parameters and crystallite sizes of $Ni_{1-x}Co_xFe_2O_4$ (where
x = 0.0, 0.1, 0.2 and 0.3) ferrites

Sample (Contents x of Co)	Obs. *a=b=c* (Å)	Cal. *a=b=c* (Å)	*D* (nm)
0.0	8.3450	8.3450	73.5475
0.1	8.3474	8.3474	70.0537
0.2	8.3532	8.3495	51.4843
0.3	8.3578	8.3578	50.2421
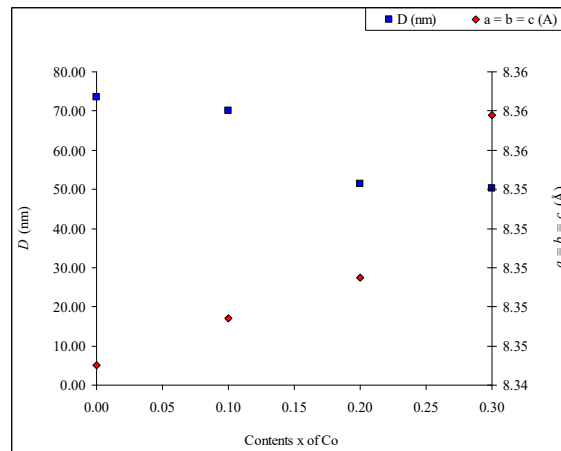
Figure 5. Variations of the lattice parameters and crystallite sizes of
$Ni_{1-x}Co_xFe_2O_4$ ferrites with the Co concentration

Microstructural Analysis

Grain size and pore structure have a major effect on the properties in polycrystalline materials. Due to the microstructure has a major role in the performance of a ceramic sensor, e.g., gas sensor, in this work, the microstructures of the end products (as-prepared ferrites) by SEM to investigate the external morphology of the grain shape, size and pore formation of the as-prepared ferrite samples. SEM micrographs of $Ni_{1-x}Co_xFe_2O_4$ (where x = 0.0, 0.1, 0.2 and 0.3) ferrites powders are shown in Figures 6(a – d).

This figures show that the samples consist primarily of irregularly shaped of 0.08 μm to 0.70 μm aggregates of fine particles. It can be seen that

the crystallite sizes of the samples are extremely fine, on the order 80 nm to 800 nm. The materials are characterized by high intergranular porosities in the observed SEM micrographs; about 20% in x = 0.0, 25% in x = 0.1, 25% in x = 0.2 and 10% in x = 0.3 of $Ni_{1-x}Co_xFe_2O_4$ samples. Furthermore, many large and large pores are present in x = 0.0, 0.1 and 0.2 samples and many large and small pores are present only in x = 0.3 sample. The grain sizes are listed in Table 3.
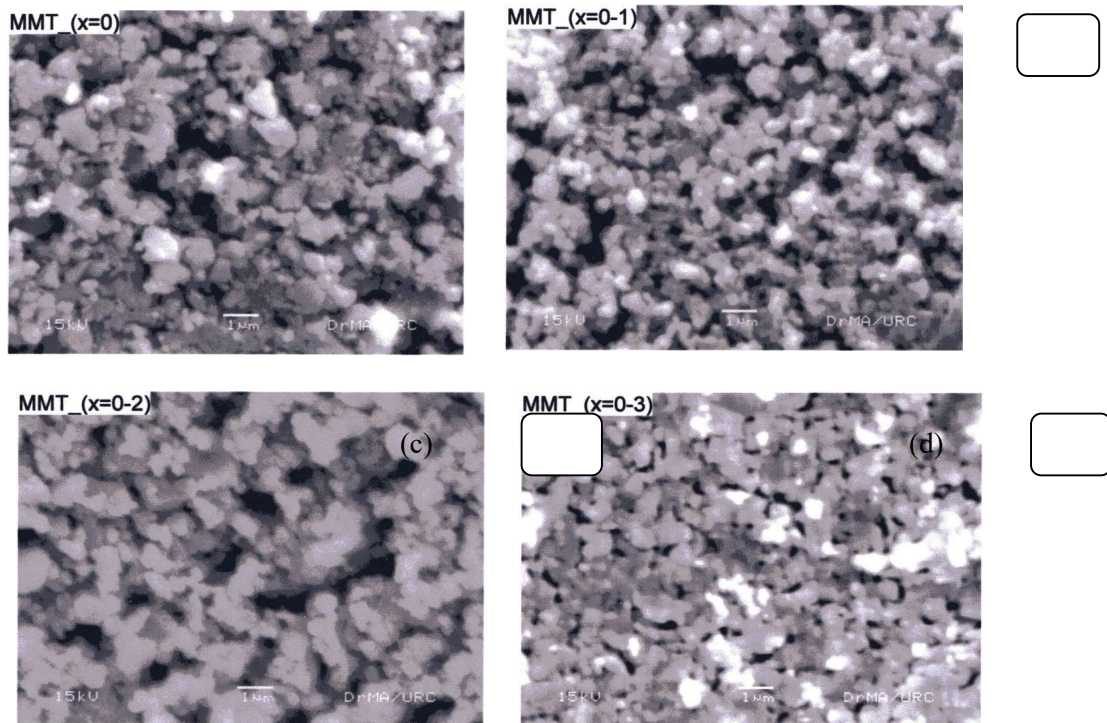
Figure 6. SEM micrograph of $Ni_{1-x}Co_xFe_2O_4$ where (a) x = 0.0, (b) x = 0.1, (c) x = 0.2 and (d) x = 0.3 ferrites

Table 3. Grain sizes of $Ni_{1-x}Co_xFe_2O_4$ (where x = 0.0, 0.1, 0.2, 0.3) ferrites

Sample (Contents x of Co)	Grain size (mm)
0.0	0.08 – 0.70
0.1	0.08 – 0.40
0.2	0.12 – 0.50
0.3	0.10 – 0.70

Gas Sensitive Electrical Property Study

The gas-sensing responses of $Ni_{1-x}Co_xFe_2O_4$ (where x = 0.0, 0.1, 0.2 and 0.3) samples to different reducing gases like acetone, ethanol, octane and liquid petroleum gas (LPG) at ambient temperature were analyzed for the applications of gas sensing materials.

In the present work, gas response characteristics of $Ni_{1-x}Co_xFe_2O_4$ ferrites in the acetone, ethanol, octane and liquid petroleum gas (LPG) atmosphere after 3 min and 5 min exposure time are depicted in Figures 7 (a – d) and Figure 8(a – d) respectively. The gas sensitivities of the samples with corresponding test gases after 3 min ($S_{3\ min}$) and 5 min ($S_{5\ min}$) exposure time are tabulated in Table 4(a – d). The most sensitive data are high-lighted in the tables.

As presented in tables, the most sensitive samples with corresponding test gases were as follows:

- For $Ni_{1-x}Co_xFe_2O_4$ (x = 0.0) ferrite after exposure times 3 min and 5 min, the most sensitive test gases are LPG and acetone.

- For $Ni_{1-x}Co_xFe_2O_4$ (x = 0.1) ferrite after exposure times 3 min and 5 min, the most sensitive test gas is LPG.

- For $Ni_{1-x}Co_xFe_2O_4$ (x = 0.2) ferrite after exposure times 3 min and 5 min, the most sensitive test gases are acetone and LPG.

- For $Ni_{1-x}Co_xFe_2O_4$ (x = 0.0) ferrite after exposure times 3 min and 5 min, the most sensitive test gases are ethanol and LPG.

It can be said that the x = 0.0 and x = 0.1 samples were the most sensitive to LPG and the other samples x = 0.2 and 0.3 were the most sensitive to acetone gas and ethanol gas after 3 min exposure time. It can also be said that the x = 0.0 or pure $NiFe_2O_4$ sample was the most sensitive to acetone gas and the other samples (x = 0.1, 0.2 and 0.3) were most sensitive to LPG gas after 5 min exposure time.

The gas sensitive processes of the samples, for example LPG sensitive process, can be discussed as follow: The reducing gas R acting on the $Ni_{1-x}Co_xFe_2O_4$ surface can be described as

$$R \text{ (gas)} \leftrightarrow R \text{ (ads)}$$

$$O^{2-} \text{ (ads)} + e^- \leftrightarrow 2O^- \text{ (ads)}$$

$$R \text{ (ads)} + O^- \text{ (ads)} \leftrightarrow RO \text{ (ads)} + e^-$$
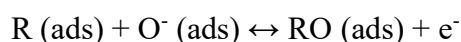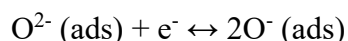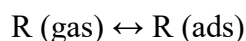
In the absence of R, electrons are removed from $Ni_{1-x}Co_xFe_2O_4$ conduction band by the reduction of O_2, resulting in the formation of O^- species and consequently the resistance of $Ni_{1-x}Co_xFe_2O_4$ sensor increases. When R is introduced, it reacts with O^- (ads) to form RO, and electrons enter the conduction band of $Ni_{1-x}Co_xFe_2O_4$ leading to decrease of resistance. The reactions, for example, involved during the butane, C_4H_{10} (LPG) sensing are summarized below:

$$C_4H_{10} \text{ (g)} + O^- \text{ (ads)} \rightarrow C_4H_8O^- \text{ (ads)} + H_2 \text{ (g)}$$

$$C_4H_8O^- \text{ (ads)} \rightarrow C_4H_8O(g) + e^-.$$
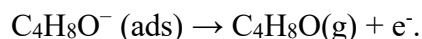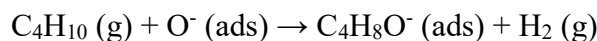
Thus, the candidate samples of Cobalt Doped Nickel ferrites, $Ni_{1-x}Co_xFe_2O_4$ (where x = 0.0, 0.1, 0.2 and 0.3) samples can be suitable applied for the LPG, acetone, ethanol and octane gas sensors.
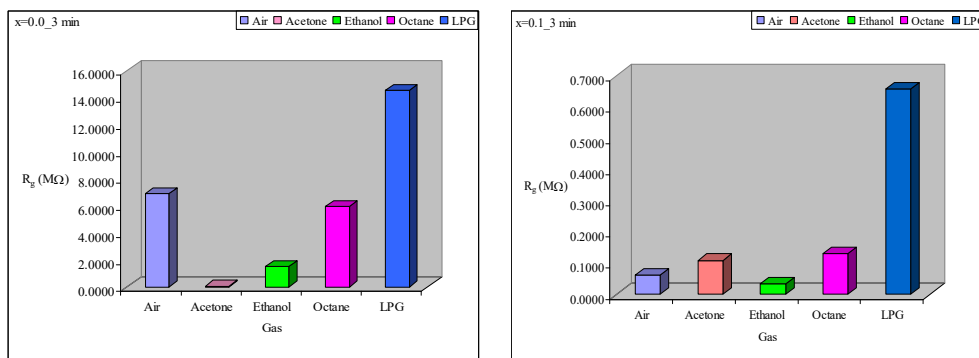
Figure 7. Gas response electrical resistances of $Ni_{1-x}Co_xFe_2O_4$ (a) x = 0.0 and (b) x = 0.1 ferrites after 3 min exposure time
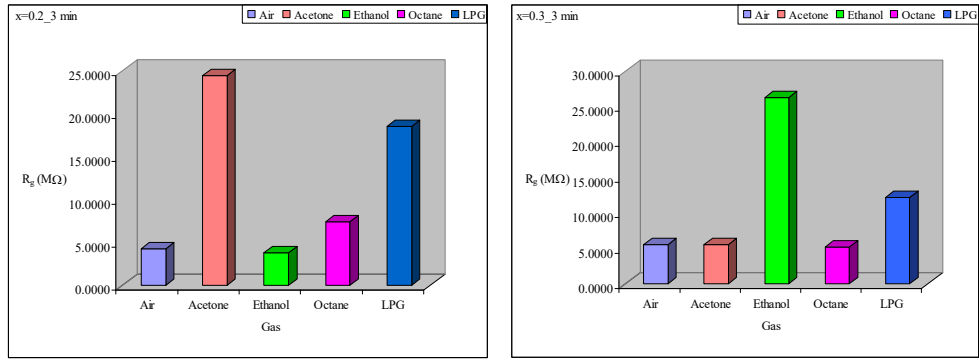
Figure 7. Gas response electrical resistances of $Ni_{1-x}Co_xFe_2O_4$ (c) x = 0.2 and (d) x = 0.3 ferrites after 3 min exposure time
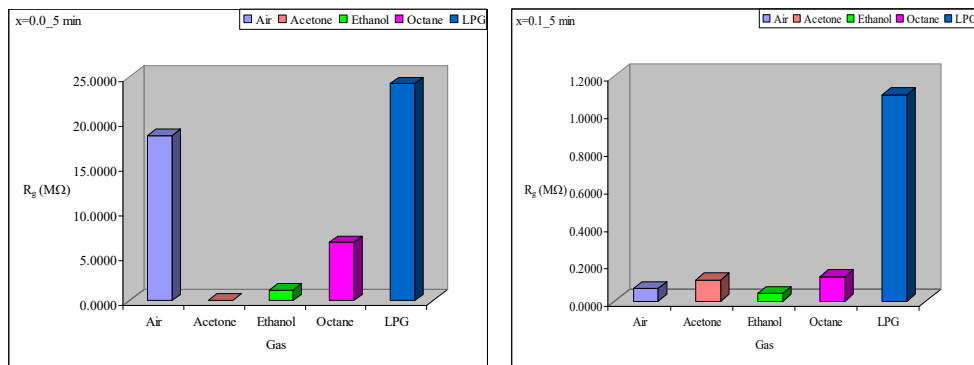
Figure 8. Gas response electrical resistances of $Ni_{1-x}Co_xFe_2O_4$ (a) x = 0.0 and (b) x = 0.1 ferrites after 5 min exposure time
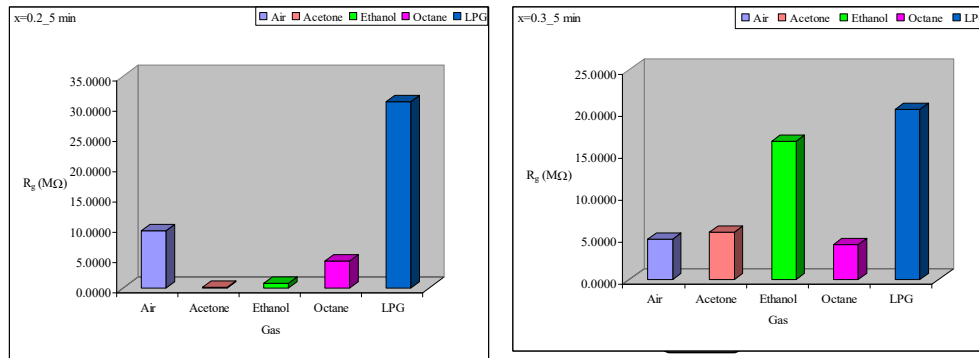
Figure 8. Gas response electrical resistances of $Ni_{1-x}Co_xFe_2O_4$ (c) x = 0.2 and (d) x = 0.3 ferrites after 5 min exposure time

Table 4.(a) Sensitivities of the $Ni_{1-x}Co_xFe_2O_4$ (where x = 0.0) sample after 3 min and 5 min exposure time

Gas	$S_{3\ min}$	$S_{5\ min}$
Acetone	0.9902	0.9962
Ethanol	0.7800	0.9344
Octane	0.1359	0.6457
LPG	1.1057	0.3139

Table 4.(b) Sensitivities of the $Ni_{1-x}Co_xFe_2O_4$ (where x = 0.1) sample after 3 min and 5 min exposure time

Gas	$S_{3\ min}$	$S_{5\ min}$
Acetone	0.7659	0.6858
Ethanol	0.4457	0.3924
Octane	1.1350	0.9379
LPG	9.7220	15.2574

Table 4.(c) Sensitivities of the $Ni_{1-x}Co_xFe_2O_4$ (where x = 0.2) sample after 3 min and 5 min exposure time

Gas	$S_{3\ min}$	$S_{5\ min}$
Acetone	4.6816	0.9835
Ethanol	0.1050	0.9166
Octane	0.7186	0.5308
LPG	3.3047	2.2749

Table 4.(d) Sensitivities of the $Ni_{1-x}Co_xFe_2O_4$ (where x = 0.3) sample after 3 min and 5 min exposure time

Gas	$S_{3\ min}$	$S_{5\ min}$
Acetone	0.0020	0.1568
Ethanol	3.7653	2.3926
Octane	0.0544	0.1337
LPG	1.2105	3.1770

Conclusion

Nanocrystalline Cobalt Doped Nickel ferrites, $Ni_{1-x}Co_xFe_2O_4$ (where x = 0.0, 0.1, 0.2 and 0.3) samples were successfully prepared by self-combustion method and their structural analysis, microstructural characteristic and gas response electrical property were reported in this work.

The X-ray diffraction patterns of the samples indicated the single-phase spinel type cubic crystalline materials. The lattice parameters of increased with increase in dopant concentration of Co on Ni ferrites in the samples. It was suggested that the lattice substitution of divalent cations of Co^{2+} on Ni^{2+} in each of the unit cell of the samples. It indicated that the presence of Co^{2+} ions causes appreciable change in the structural properties of $Ni_{1-x}Co_xFe_2O_4$. The obtained average crystallite sizes showed the nanocrystalline nature of the materials. SEM micrographs indicated that the grains were high intergranular porosities. The pores serve as adsorption sites due to the decomposition of starting materials in the preparation of candidate materials with poor grain boundary. It can also be found that in each of the SEM micrographs, many large and large pores are present in x = 0.0, 0.1 and 0.2 samples and many large and small pores are present only in x = 0.3 sample. The obtained grain sizes are in the range 0.08 μm to 0.70 μm. From the test gas response and the obtained sensitivities results, the following facts were proposed for the applications of the candidate materials:

- For $Ni_{1-x}Co_xFe_2O_4$ (x = 0.0) ferrite after the exposure times 3 min and 5 min to the best sensitive gases are LPG and acetone.
- For $Ni_{1-x}Co_xFe_2O_4$ (x = 0.1) ferrite after the exposure times 3 min and 5 min to the best sensitive gas is LPG.
- For $Ni_{1-x}Co_xFe_2O_4$ (x = 0.2) ferrite after exposure times 3 min and 5 min to the best sensitive gases are acetone and LPG
- For $Ni_{1-x}Co_xFe_2O_4$ (x = 0.3) ferrite after exposure times 3 min and 5 min to the best sensitive gases are ethanol and LPG respectively.

According to experimental results, the samples can be used for the applications of gas sensors with the corresponding test gas. Most of the samples should be used for LPG gas sensor. Especially, only the x = 0.1 sample is the most suitable for the application of LPG sensor.

Acknowledgement

References

1. Harris, V.G., Geiler, A., Chen, Y., Yoon, S.D., Wu, M., Yang, A., Chen, Z., He, P., Parimi, P.V., Zuo, X., Patton, C.E., Abe, M., Acher O. & Vittoria, C. (2009). Recent advances in processing and applications of microwave ferrites. *Journal of Magnetism and Magnetic Materials*, 321, pp. 2035-2047.

2. Iyer, R., Desai, R. & Upadhyay, R.V. (2009). Low temperature synthesis of nanosized $Mn_{1-x}Zn_xFe_2O_4$ ferrites and their characterizations. *Bulletins Materials Science*, 32, pp.141-147.

3. Kumar, N., Kumar, V., Arora, M., Sharmar, M., Singh, B. & Pant, R.P. (2009). Synthesis of $Mn_{0.2}Zn_{0.8}Fe_2O_4$ particles by high energy ball milling and their applications *Indian Journal of Engineering and Materials Science*, 16, pp. 410-414.

4. Marial, K.H., Choudhury, S. & Hakim, M.A. (2013). Structural phase transformation and hysteresis behavior of Cu-Zn ferrites. *International Nano Letters*, 3, 1-10.

5. Pathan, A.N., Sangshetti, K. & Pangal, A.A.G. (2010). Synthesis and Moussbauer Studies on Nickel-Zinc-Copper Nanoferrites. *Nanotechnology and Nanoscience*, 1(1), 13-16.

6. Sharma, R.K., Suwalka, O., Lakshmi, N., Venugopala, K., Banerjee, A. & Joy, P.A. (2005) Synthesis of Chromium Substituted Nano Particles of Cobalt Zinc Ferrites by Coprecipitation. *Materials Letters*, 59, 3402-3405.